Low Temperature Physics/Fizika Nizkikh Temperatur, 2020, v. 46, No. 3, pp. 346–354

Comparison of temperature dependences of electrical conductivity of composite rGO-SWNT film with rGO and SWNT films

N.V. Kurnosov, A.S. Linnik, and V.A. Karachevtsev

B. Verkin Institute for Low Temperature Physics and Engineering of the National Academy of Sciences of Ukraine
47 Nauky Ave., Kharkiv 61103, Ukraine
E-mail: karachevtsev@ilt.kharkov.ua

Received November 7, 2019, published online January 27, 2020

Temperature dependences of electrical conductivity of reduced graphene oxide composite with single-walled nanotubes (rGO-SWNTs) and rGO films has been studied in the temperature range of 25–290 K. Both films were obtained by vacuum filtration of aqueous suspensions. Temperature dependences of conductivity of films were found similar to the conductivity observed in disordered semiconducting systems. It was demonstrated that the behavior of the conductivity temperature dependence of pure rGO, SWNTs and composite film is different. The temperature dependences of the resistance $R(T)$ of the films were analyzed within the framework of the variable range hopping (VRH) transport in which electron motion is due to the thermo-activated quantum tunneling between localized states. Two-dimensional Mott VRH (Mott 2D VRH) and Efros–Shklovskii VRH (ES VRH) models were applied for analysis. Mott 2D VRH was observed for rGO-SWNT film in the interval of 25–200 K. At higher temperatures $R(T)$ of rGO-SWNT was fitted with Arrhenius-like equation describing electron activation from localized states to delocalized ones. $R(T)$ of the rGO film followed the Mott 2D VRH model from 165 to 290 K, however, at lower temperatures ES VRH model was exploited. From approximation of $R(T)$ by these models the parameters of the electron transport in rGO-SWNT and rGO films were estimated. It was suggested that nanotubes in rGO-SWNT composite serve as conductive bridges among rGO sheets enhancing the conductivity as compared to rGO. The conductivity of rGO also influences on the composite properties because 2D character of electron motion is kept in sharp contrast to SWNT film which demonstrated three-dimensional Mott VRH electron transport in the same temperature range.

Keywords: low-temperature electrical conductivity, disordered systems, reduced graphene oxide, single-wall carbon nanotube, reduced graphene oxide-carbon nanotube hybrids, variable range hopping conductivity.

1. Introduction

Graphene nanomaterials have attracted great interest in the last years due to unique optical, mechanical, thermal and electrical properties [1]. Among them electrical properties received considerable response in real applications as these materials open new pathways for the improvement of existing technologies such as sensoring, fabrication of new electronic devices, production of supercapacitors and lithium batteries, layering conductive and transparent coverage and so on (see, for example, Ref. 2 and references therein). Functionalization of graphene with oxygen-containing groups creates a novel material — graphene oxide (GO) which expands the practical applications of graphene. One of the main advantages of GO is its dispersibility in water, which facilitates the production of graphene nanomaterials in industrial volumes. Graphene oxide can be prepared in large scale through chemical exfoliation method of graphite, however, GO is an electrically insulating material. Electrical properties of GO can be changed through controlled chemical/thermal reduction processes. The reduced graphene oxide (rGO) is composed of nanometer-sized conducting sp^2 domains alternated with insulating highly disordered sp^3 regions formed by oxygen functional groups. The charge transport behavior of rGO is quite different from that of graphene, where ballistic electron transport over several microns was observed [3].

Elaboration of hybrids and composites based on graphene nanomaterials allows to overcome disadvantages of GO in conductivity. First of all, hybrids of GO/rGO with carbon nanotubes (CNTs) are appropriate for this cause. CNTs are randomly distributed between rGO or GO sheets

and provide a high mechanical strength and flexibility of such films also increasing conductivity between rGO/GO sheets, since CNTs have high electrical conductivity and can closely contact with the graphene surface [4]. Applications mentioned above require good understanding of the conduction mechanisms in these disordered nanomaterials. It is also necessary to obtain detailed information about localized/mobile electron states, to estimate the role of structural defects and to understand how we can tune electrical properties through GO reduction.

Previous measurements of electrical transport have shown that the rGO exhibits a semiconductor behavior with a negative temperature coefficient of resistance. Research on the electrical characteristics showed that at low temperatures the charge transport in rGO is mainly described by thermally activated tunneling in terms of variable-range hopping (VRH) model proposed by Mott [5] and fluctuation-induced quantum tunneling (FIT) model elaborated by Sheng [6,7]. Two-dimensional (2D) Mott VRH law was applied for fitting the temperature dependences of resistance of the rGO monolayer and the thin rGO sheets within 4–298 K range [8]. Kaiser *et al.* [9] have also performed a detailed study of the electrical conduction process in individual monolayers of rGO down to a temperature of 2 K. The observed conductance was explained in the framework of Mott 2D VRH model with electron tunneling between localized sp^2 states. Eda *et al.* [10] also applied the Mott 2D VRH model to individual rGO sheets with different degrees of reduction to describe the electron transport from 78 to 240 K. A deviation from this model observed above 240 K for the well-reduced rGO flakes was explained by the thermally activated conduction mechanism that dominated in the high-temperature range (Arrhenius law). Two mechanisms were proposed for electrical conduction in chemically reduced rGO thin films studied in a wide range (50 K < T < 400 K) of temperatures: at higher temperatures, Arrhenius-like temperature dependence of resistance was observed while at lower temperatures the rGO sample showed a conduction mechanism consistent with Mott 2D VRH model [11].

Experimental results on the charge transport in GO film studied at various temperatures from 300 to 120 K were also matched with Mott 3D VRH model [12]. In another study at electrical transport measurement in chemical reduced rGO film from 20 to 297 K indicates the carrier transport mechanism is thermally activated band conduction above 200 K and 3D Mott's variable range hopping below 100 K [13].

In a few works Efros–Shklovskii VRH (ES VRH) model is exploited for fitting the temperature-dependent charge transport in rGO films [14,15], monolayer graphene [16] and hydrogenated graphene [17]. In the framework of this model Coulomb interaction between electron and hole is not negligible that leads to a power-law dependence of density of states (DOS) on energy near Fermi level ε_F [18,19]. Energy interval E_{CG} with gradually vanishing density of states is called Coulomb gap.

D. Joung and S.I. Khondaker [14] investigated the low-temperature electron transport properties of chemically reduced rGO sheets with different carbon sp^2 fractions (ranged from 55 to 80%). They showed that the temperature-dependent resistance of all the samples follows ES VRH model. Chuang *et al.* [17] performed transport measurements on a hydrogenated graphene sheet in the temperature range of 4.5–45 K. They also demonstrated that ES VRH is the dominant transport mechanism in that system.

It was proposed that for samples with the high disorder ES VRH mechanism dominates at all measurable temperatures. In other relatively low disordered samples, the energy scale is such that the carriers may have enough energy to overcome E_{CG} at all temperatures, and, in that case, only Mott VRH can be applied [14]. At intermediate disorders, it may be possible to observe a crossover from ES to Mott VRH with increasing temperature in the sample. Such phenomenon was reported in Refs. 15, 17, the authors also discussed the relation between crossover temperature and the Coulomb gap energy E_{CG}.

Recently temperature-dependent charge transport behavior was investigated in thick rGO film [20]. It was shown that charge transport occurs through two parallel percolating conducting pathways. For large disordered regions conductance is determined dominantly by Mott 3D VRH while for small and medium disordered regions and crystalline sp^2 domains its conductance is determined by quantum tunneling (FIT model) and thermal activation.

The electrical conductivity in thin layers of GO(rGO)-SWNT (single-walled nanotube) hybrids is analyzed only in few works [21,22]. The electrical conductivity in such composite films is mainly conditioned by SWNTs, since they serve as conductive bridges for charge carriers between non-conducting rGO sp^3 domains. V. Skakalova and coauthors [21] had shown that the presence of electrically insulating GO within the SWNTs network significantly enhances its electric conductivity, while rGO suppresses electrical conductivity in a composite network with SWNTs. In our recent work [22] we have studied the low-temperature (5–290 K) electronic transport in composite film of GO-SWNTs obtained by vacuum filtration of their aqueous suspension. The temperature dependences of the resistance $R(T)$ of the films were analyzed within the framework of the Mott 3D VRH model describing the electron transport in the interval of 5–240 K. From the analysis of these dependences, the parameters of the electron transport (the mean length and energy of the electron hopping) in the GO-SWNTs and in the SWNTs films were estimated. Arrhenius equation was involved to describe the temperature dependence of the resistance of films at T > 240 K. The averaged potential barrier value obtained in approximating $R(T)$ with the Arrhenius formula was larger for composite compared to SWNT film (18 vs 11 meV). The comparison of the parameters obtained for different films showed that contact of nanotubes with GO surface complicates the electron transport in composite film.

As we can see, the different mechanisms with two- or three-dimensional transport behavior are involved to understand the electron transport in GO (rGO) structures at low temperatures. Such multifarious behavior can be partly explained by different reduction degree of rGO, variety of linear and volume sizes of rGO flakes, different arrangement of flakes depending on the film preparation and so on. In composite this picture obtains additional variety due to heterogeneity of nanotube component. In this respect, additional fundamental research is much needed in this direction.

In this work we have analyzed the temperature dependence of resistance of composite rGO-SWNT film and compared this dependence with that of rGO and SWNT films in the temperature range of 25–290 K. Films obtained by vacuum filtration from aqueous suspension of rGO and rGO-SWNT hybrids (weight ratio 1:1) were rather thick (up to 10 μm thick), SWNTs used for composite preparation had prevailing semiconducting nanotubes (~95%) content. Mott 2D VRH model was applied for fitting the $R(T)$ dependence of composite film in the interval of 25–200 K while for higher temperatures $R(T)$ dependence follows the Arrhenius law. rGO film demonstrates $R(T)$ dependence that has different behavior compared to composite film: for lower temperature range (25–165 K) ES VRH model was applied and for higher one Mott 2D VRH formula was used.

2. Experimental details

Materials. The reduced graphene oxide (fraction of carbon ~87%) was purchased from Graphenea company (San Sebastian, Spain) and single-walled carbon nanotubes synthesized by chemical vapour deposition CoMoCAT method (SouthWest Nanotechnologies, USA) were used in experiments. The SWNTs contained predominantly semiconducting nanotubes (~ 95%), among them, nanotubes of chirality (6.5) prevailed.

Preparation of rGO-SWNT hybrids in aqueous suspensions and films. The composite rGO-SWNTs film was obtained from aqueous suspension of rGO-SWNTs (0.5–2 ml) deposited on the PTFE membrane (diameter 12.5 mm, pores 0.24 μm, Millipore, USA) by vacuum filtration. Preparation of aqueous suspension was based on ultrasound treatment (60 min, 22 kHz) with following centrifugation (3000*g*, 15 min) of rGO and SWNTs with 1:1 weight ratio. The rGO film was obtained similarly. The rGO-SWNT or rGO films were then separated from the membrane to obtain circle-shaped films as a result (diameter ~9 mm, thickness 4–10 μm).

Low-temperature measurements of electrical conductivity. The low-temperature measurements in the range of 25–290 K were carried out in a helium cryostat with samples kept in the gas helium atmosphere. The samples were film stripes 0.4–1.5 mm wide attached between contacts distanced at 3 mm, the average rate of temperature changes was about 1.5–2 K/min. Measurements of resistance were performed for rGO and rGO-SWNT samples simultaneously, during both cooling and heating courses. No resistance hysteresis was found.

3. Results and discussion

3.1. Temperature dependences of conductivity/resistance of the rGO-SWNT composite, rGO and SWNT films

In the low-temperature experiments we have measured the resistance of rGO-SWNT and rGO films and obtained the dependences of resistance on temperature in the range of 25–290 K. $R(T)$ dependences of two films are shown in Fig. 1. Both films exhibit gradual increase of R at T lowering. The changes are more pronounced in case of rGO sample, R is increased by a factor of 60, while for composite rGO-SWNT the R value is only increased ~6 times. Note that in the whole temperature range the resistance of the composite film is about two orders of magnitude lower than in rGO film.

More noticeable difference in temperature behavior of the charge transport of the rGO and rGO-SWNT films can be observed in Fig. 2 where the temperature dependences of the conductivity (σ) (normalized to value at 290 K) are plotted. The $\sigma(T)$ of SWNT film reported earlier [22] is shown in Fig. 2(a) too. The decrease of the conductivity with lowering of temperature indicates that this dependence is similar with the conductivity observed in disordered semiconducting systems.

Conductivity derivative $d\sigma/dT$ for these three samples was also calculated in order to characterize the rate of conductivity change with temperature (Fig. 2(b)). It is obvious that the conductivity temperature dependence of rGO differs largely from the dependences of rGO-SWNT and SWNT films which are rather similar. The conductivity of rGO film decreases almost linearly from room temperature

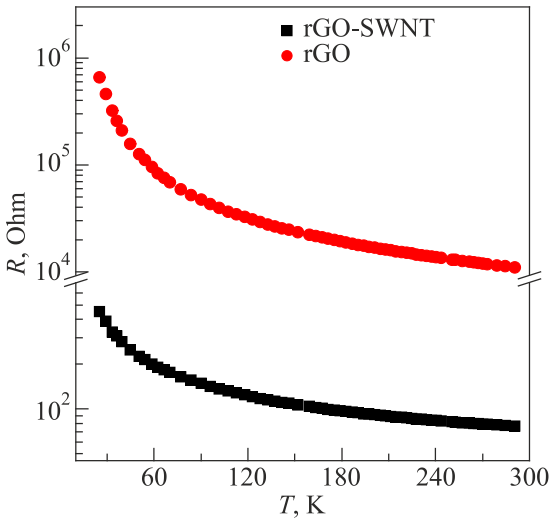

Fig. 1. The resistance temperature dependences plotted for rGO-SWNT (squares) and rGO (circles) films.

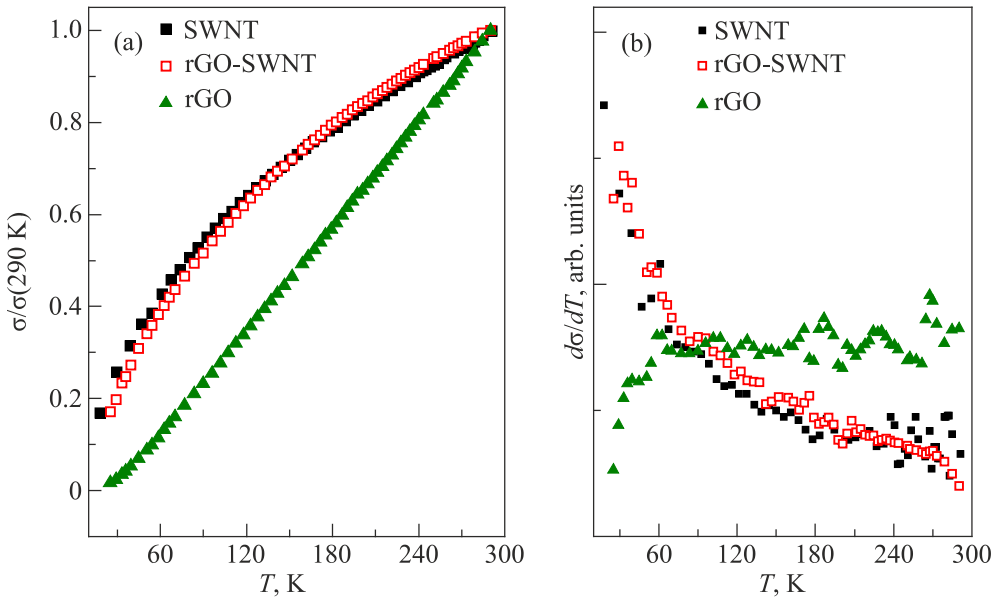

Fig. 2. Conductivity temperature dependences for SWNT [22] (full squares), rGO-SWNT (open squares) and rGO (triangles) films normalized to the value at 290 K (a). Temperature dependences of conductivity derivatives $d\sigma/dT$ for SWNT, rGO-SWNT and rGO samples (b).

to ~60 K yielding constant $d\sigma/dT$, then starting from ~60 K down to 25 K there is pronounced decrement of $d\sigma/dT$ (see Fig. 2(b)). No such tendency was observed in case of rGO-SWNT or SWNT films, on the contrary, $d\sigma/dT$ is increases at lowering temperature. Such behavior can indicate the different mechanisms of electron transport in rGO and composite rGO-SWNTs (or SWNT) films.

Therefore the next step in our investigation was aimed to elucidate which electron transport models are applicable for our samples in the temperature range of 25–290 K. As our films can be considered a disordered semiconducting systems we should analyze the temperature dependences of the resistance $R(T)$ within the framework of model involving thermo-activated tunneling through barriers between localized states with a variable range hopping (model VRH). In order to clarify this we have analyzed the $R(T)$ dependences of films by logarithmic derivative evaluation which was used earlier for similar systems [14,15,17].

The main idea of such procedure is that it can provide self-consistent and unambiguous evaluation of power parameter m in the general formula of resistance that can be derived in hopping conductivity transport [5,19]:

$$R \sim \exp\left[(T_0 / T)^m\right], \tag{1}$$

where $0 < m < 1$. First, we define reduced activation energy $W = -\partial \ln R(T) / \partial \ln T$. Then we plot its logarithm versus logarithm of temperature, as is shown in Fig. 3 for both rGO and rGO-SWNT films. Lastly, a linear fitting of calculated data points is performed for each sample (up to the temperatures indicated by arrows in Fig. 3). Such fitting includes parameter m:

$$\ln W = A - m \ln T. \tag{2}$$

As a result of the fitting, we obtain $m = 0.5 \pm 0.02 \approx 1/2$ in the range of 25–163 K in case of rGO film and $m = 0.34 \pm 0.02 \approx 1/3$ in the range of 25–197 K for the composite rGO-SWNT film. It should be noted that within Mott VRH model parameter m in Eq. (1) is directly related to the dimensionality d of hopping conductivity:

$$m = \frac{1}{1+d}. \tag{3}$$

So, $d = 2$ suggests applicability of Mott 2D VRH transport model for the rGO-SWNT in the lower temperature range. But although formula (3) is correct in Mott mo-

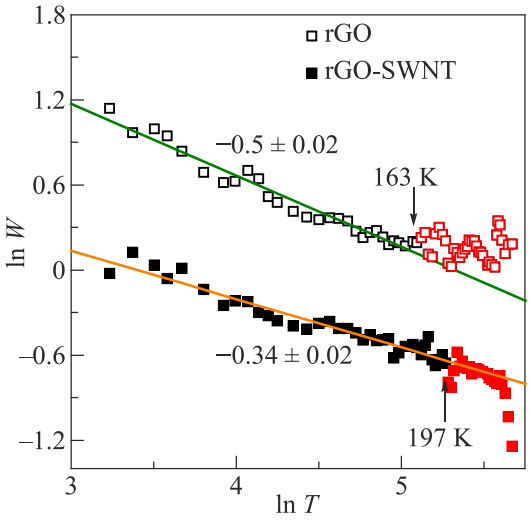

Fig. 3. (Color online) Logarithm of reduced activation energy W plotted vs logarithm of temperature T for the rGO (open squares) and rGO-SWNT (full squares) films. Linear fits and resulting slopes are shown. Arrows indicate the high-temperature margins of linear fits.

del, it is widely accepted in case of graphene-related systems that evaluated $m \approx 1/2$ does not mean one-dimensional ($d = 1$) Mott VRH, but rather Efros–Shklovskii hopping conductivity (ES VRH). ES VRH model was used in Refs. 14–17 to describe temperature dependence of conductivity (or resistance) in rGO and graphene samples including those with different degree of reduction and disorder.

3.2. The temperature dependences of electron transport in the rGO-SWNTs and SWNTs films: Mott VRH and Arrhenius models

In this section we discuss the rGO-SWNT composite film transport properties and also make a comparison with composite containing strongly oxidized graphene oxide (GO-SWNT) and nanotube film (SWNT) [22]. As was shown in previous section, the logarithmic derivative evaluation for rGO-SWNT yielded $m = 1/3$ in Eq. (1) which means that Mott 2D VRH is the mechanism of electron transport. An additional confirmation is provided when $R(T)$ dependence of rGO-SWNT is plotted in $\ln R$ vs $T^{-1/3}$ coordinates (see Fig. 4(a)) which should transform Eq. (1) into linear equation. Obtained data indeed can be well fitted linearly at least from 25 up to 197 K.

The 2D character of Mott VRH in case of rGO-SWNT is the main difference from GO-SWNT and SWNT samples which both exhibited Mott 3D VRH (see Ref. 22 for details). Resulting two-dimensionality of electron transport in rGO-SWNT can be due to the rather important role of rGO sheets present in the film. rGO is a conductive 2D material and can contribute to electron transport in composite, while strongly oxidized GO film had no measurable conductivity. Therefore electron transport in GO-SWNT composite was largely conditioned by SWNT bundle network, which was non-oriented and "isotropic" yielding 3D VRH.

We have also noted that starting from ~200 K towards higher temperatures there is a small deviation between experimental data and linear fit for the rGO-SWNTs sample. This is shown in detail in Fig. 4(b). We assume that in the range of ~200–290 K the activation transport mechanism which yields Arrhenius-like equation (4) for the resistance:

$$R \sim \exp\left(T_a / T\right) \tag{4}$$

is more precise for our composite film. Parameter T_a in case of disordered systems describes the averaged separation between the localized states (which contribute to VRH processes) and delocalized states. Such mechanism takes place if thermal energy is large enough to overcome the energy barriers that define potential wells where states are localized. Experimental data in the range of 201–290 K plotted in $\ln R$ vs T^{-1} coordinates and linear fit are shown in Fig. 5(a). In addition, we provide the $R(T)$ dependence in the same temperature range (Fig. 5(b)) to demonstrate that curve calculated using Eq. (4) fits to the experimental data well. At the same time the lower temperature data of the resistance dependence follows the Mott 2D VRH curve which corresponds to Eq. (1) at $m = 1/3$.

The evaluated T_a parameter was 115 K which is reasonably lower than the temperature in the fitted range. Therefore at higher temperatures (> 200 K) the thermal energy is sufficient for activation transport mechanism. Interestingly, the T_a for the rGO-SWNT is only slightly lower than that obtained for the SWNT sample (130 K) [22]. This may indicate that transport through SWNTs is dominant at high temperatures for rGO-SWNT composite. Also, if we compare T_a for composites containing GO with different oxidation degree (rGO-SWNT and GO-SWNT), we conclude that T_a is much larger in case of GO-SWNT (212 K) [22]. This means that non-conductive strongly oxidized GO sheets

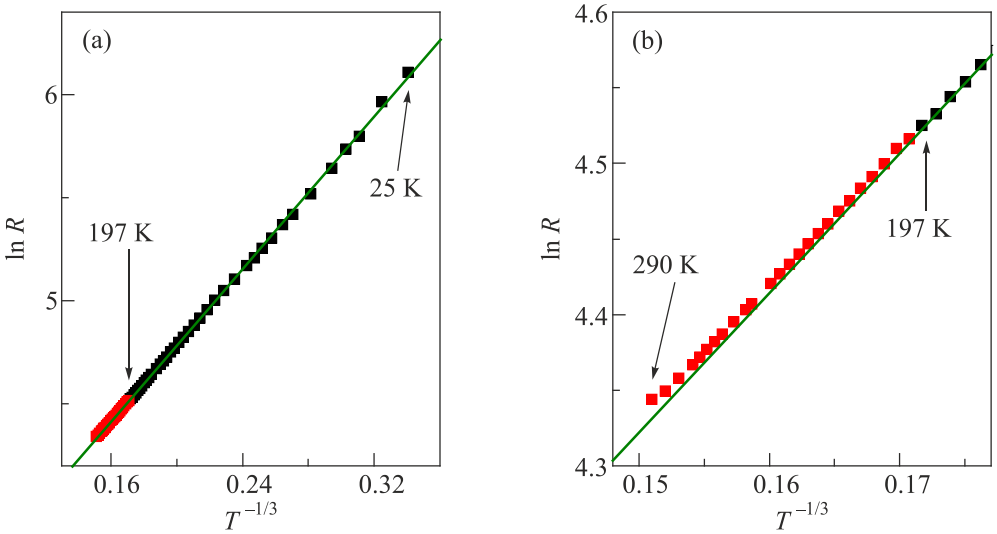

Fig. 4. (Color online) Semilogarithmic plots of $\ln R$ vs $T^{-1/3}$ for the rGO-SWNTs film in the range of 25–290 K (a) and 183–290 K (b). The marginal temperatures for linear fit in (a) are indicated by arrows.

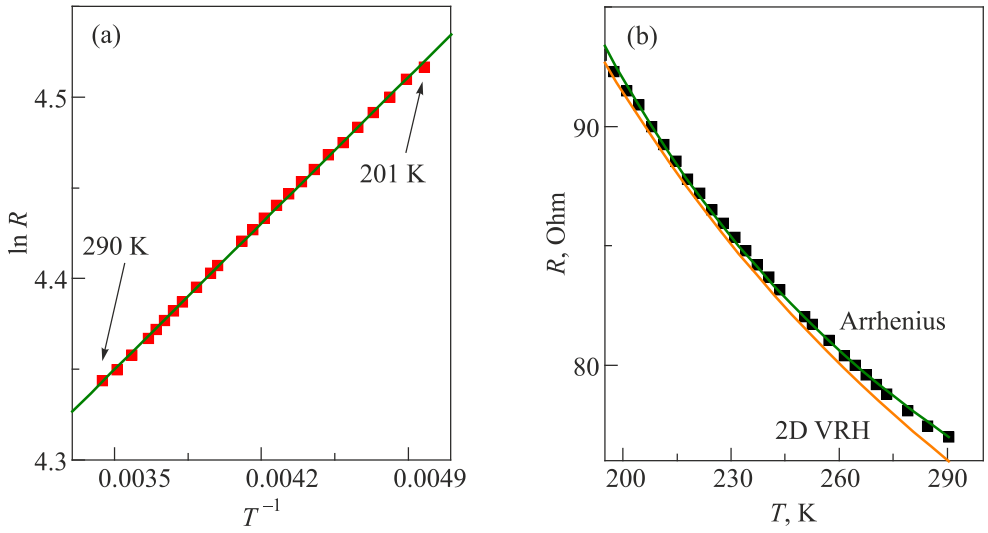

Fig. 5. Dependences of $\ln R$ on T^{-1} (a) and R on T (b) in the temperature range of ~200–290 K plotted for the composite rGO-SWNT film.

increase the potential barriers in composite film in contrast to conductive rGO sheets.

3.3. The temperature dependence of electron transport in the rGO film: ES VRH and Mott 2D VRH models

Results of fitting presented in Fig. 3 allow us to claim that the ES VRH model is applicable for electron transport in our rGO sample at low temperatures. The key feature of ES VRH model is consideration of Coulomb interaction for tunneling charges. It is interaction between electron in the final state (the one which electron occupies after tunneling event) and hole which is left in the initially occupied state. This interaction changes the density of states distribution along energy scale. While in Mott model density of states near Fermi level (i.e., localized states which contribute to tunneling) is supposed constant, in ES VRH model this density of states depends on energy and comes to zero at Fermi level:

$$N(\varepsilon) \sim |\varepsilon - \varepsilon_F|^n . \tag{5}$$

The energy range E_{CG} in which Eq. (5) is correct is called Coulomb gap. Efros and Shklovskii had shown that parameter n depends on dimensionality (n = 2 in 3D transport and n = 1 in 2D transport) [19], and the resulting formula for the resistance temperature dependence yields:

$$R \sim \exp[(T_{ES}/T)^{1/2}]. \tag{6}$$

This formula was applied to approximation of the experimental results obtained for rGO sample. It was previously concluded that ES VRH conductivity model is applicable up to 163 K (linear fit in Fig. 3 yielded m = 1/2 in Eq. (1)). On the other hand, the higher temperature data in Fig. 3 (starting from point 167 K) cannot be well fitted in $\ln W$ vs $\ln T$ plot and m for this range was not evaluated. So we have analyzed the $R(T)$ dependence of rGO film using $\ln R$ vs $T^{-1/2}$ and $T^{-1/3}$ coordinates as is shown in Figs. 6(a), (b), respectively.

Data in Fig. 6(a) also gives additional evidence for ES VRH model in 25–163 K range. But approximately near 165 K the experimental data start to deviate from linear fit in $\ln R$ and $T^{-1/2}$ coordinates. In order to obtain linear fit for the higher temperature data we should use the $\ln R$ and $T^{-1/3}$ coordinates (Fig. 6(b)) meaning power parameter $m \approx 1/3$ in Eq. (1). This allows us to state that approximately from 165 K up to room temperature the transport model is not ES VRH, but Mott 2D VRH. Such transition from ES to Mott VRH mechanisms for graphene and rGO samples was reported earlier [15,16]. The reason behind it is the increasing thermal energy so that tunneling occurs between the localized states positioned on energy scale outside the Coulomb gap where density of states practically does not change.

The linear fit performed for the data presented in Fig. 6(a) resulted in evaluation of ES VRH model parameter T_{ES} (see Eq. (6)), T_{ES} = 794 K. The formula for this characteristic temperature is (Gauss unit system) [19]

$$T_{ES} = \frac{2.8e^2}{k_B \kappa \xi}, \tag{7}$$

where κ is a dielectric constant of graphene, ξ is the localization length (parameter describing localized states wave function decay). Following Eq. (7) and assuming κ = 3.5 for rGO [14], we have calculated the localization length ξ = 16.8 nm (roughly equal to value reported in Ref. 15 while larger than those in Ref. 14). Note that this localization length is for states near Fermi level (inside Coulomb gap). The estimation of band gap for rGO $E_g \approx \hbar v_F / \xi$ using Fermi velocity $v_F = 10^6$ m/s [14] gave a value of $E_g \approx 0.039$ eV. The obtained E_g and ξ values suggest rela-

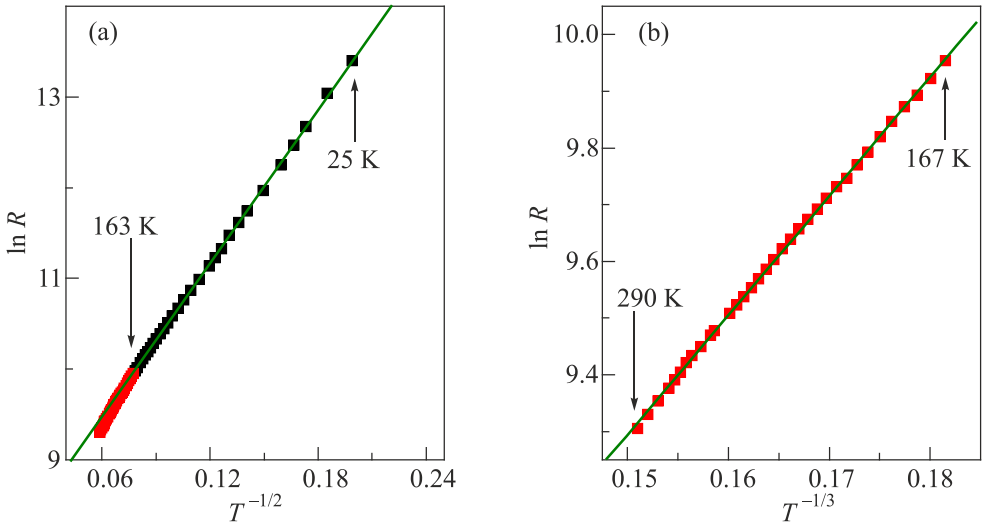

Fig. 6. (Color online) Semilogarithmic plots of ln R vs $T^{-1/2}$ (a) and $T^{-1/3}$ (b) for the rGO film. The marginal temperatures for linear fits are indicated by arrows.

tively large sp^2 domains in our sample (sized about ξ) and also mean that rGO is strongly reduced. Nevertheless, the band gap expressed in Kelvins yields 452 K and this significant value explains the absence of activation transport mechanism (4) for rGO film studied in the whole temperature range 25–290 K.

If we compare the results obtained for two films, the notable feature is the absence of ES VRH transport model for description of conductivity of rGO-SWNTs, in contrast to rGO sample where ES VRH model is confirmed. We suppose that this is strongly related to addition of SWNTs (including ~5% of metallic ones) and formation of composite, because it can alter the route of charge transport and change the distribution of density of the states near Fermi level resulting in very small (comparing to thermal energy) or even absent Coulomb gap. In this case Mott 2D VRH will be dominant at relatively low temperatures, which we experimentally observed for rGO-SWNT.

We can also analyze in our comparison the parameters that are included in ES or Mott VRH models applied to $R(T)$ dependences of rGO and rGO-SWNT films. The Mott 2D VRH was observed for both samples, so we compare the T_0 parameters (see Eq. (1)) obtained within this model. T_0 in case of 2D transport is defined by equation [19]

$$T_0 = T_M = \frac{13.8}{k_B N \xi^2}, \tag{8}$$

where N is a density of states that contribute to tunneling events, ξ is the localization length of these states. The Mott model presumes N to be constant (without dependence on energy) and equal to density of states at Fermi level $N(\varepsilon_F)$. T_M was evaluated from linear fitting performed for ln R vs $T^{-1/3}$ data in Figs. 4(a) and 6(b), resulting T_M = 790 K for rGO-SWNT composite and T_M = 9314 K for rGO film. Similarly to [22] we confirm smaller T_M for sample with larger conductivity. According to Eq. (8), decrease of T_M is caused by increase of both ξ and N (namely, $N\xi^2$ is by an order of magnitude larger for rGO-SWNT). Larger density of states and their "overlapping" (due to increased ξ) means that tunneling becomes more probable and conductivity is increased, which is experimentally observed for rGO-SWNT film. This again can be attributed to presence of intrinsically more conductive (comparing to rGO) SWNTs in composite.

We can also provide an estimation of density of states that contribute to Mott 2D VRH in rGO sample. The localization length ξ calculated using Eq. (7) can be substituted into Eq. (8) as well as T_M = 9314 K. The resulting density of states is $N = 6 \cdot 10^{12}$ eV^{-1}·cm^{-2}. But we should consider that states contributing to Mott VRH are located farther from ε_F and can have different ξ compared to those in Coulomb gap range. Therefore it is more correct to estimate density of states in the energy range where Mott 2D VRH model is observed as ~10^{12}–10^{13} eV^{-1}·cm^{-2}. Similar value was obtained earlier for rGO by Eda *et al.* [10]. Finally, we can determine the Coulomb gap width E_{CG} for rGO film according to formula [15]

$$E_{CG} = \frac{T_{ES}}{\beta\sqrt{4\pi}}. \tag{9}$$

Here β is a numeric constant, which should be equal to that used in Eq. (7). Substitution of previously evaluated T_{ES} yields the value of E_{CG} as 80 K. E_{CG} is approximately twice smaller than temperature 165 K at which we observe the transition from ES VRH to Mott 2D VRH. Such ratio between transition temperature and width of Coulomb gap is fully similar to data reported in [15] and is understandable as transition to Mott VRH should occur at $T > E_{CG}$ when Coulomb interaction becomes smaller than thermal energy.

4. Conclusion

In this work we have experimentally obtained temperature dependences of electrical resistance $R(T)$ in the range of 25–290 K for reduced graphene oxide (rGO) film and composite rGO-SWNT film containing rGO and single-walled carbon nanotubes (SWNTs). The synergistic effect is present as the composite film containing both rGO and SWNTs exhibited conductivity increased by approximately two orders of magnitude as compared to rGO film. Both films demonstrated decrease of conductivity (increase of resistance) towards low temperatures which is similar to disordered semiconducting systems.

In order to approximate the experimental $R(T)$ data we have proposed two variable range hopping (VRH) electron transport models, namely, Mott VRH and Efros–Shklovskii VRH. Both models involve electron tunneling between localized states as the mechanism of charge transport. ES VRH was proved to be the case for rGO film in the temperature range of 25–165 K while at higher temperatures two-dimensional (2D) Mott VRH transport was observed. At the same time, for the composite rGO-SWNT film ES VRH was absent and Mott 2D VRH was dominant from 25 to 200 K. We have provided evidence that at higher temperatures the activation transport mechanism takes place in composite film described by Arrhenius-like equation.

By fitting the experimental $R(T)$ dependences we have evaluated the parameters included in Mott 2D VRH and ES VRH models and calculated such physical values as localization length and density of localized states, also the Coulomb gap width (for rGO film). The performed analysis suggests that density of states outside Coulomb gap which contribute to Mott 2D VRH and their localization length are larger in case of rGO-SWNT film. This is a reason for increased conductivity of composite and it was related to presence of SWNTs that, firstly, act as additional conductive bridges between rGO sheets, secondly, provide additional charge states.

The comparison of electron transport in rGO-SWNT composite with transport in GO-SWNT composite containing practically non-conductive graphene oxide revealed difference in VRH dimensionality. In latter case three-dimensional Mott VRH transport was observed (similarly to SWNT film) and conductivity was largely conditioned by nanotubes. As for the rGO-SWNT composite, we have proved that SWNTs increase conductivity, but 2D character of resulting electron transport is kept presumably due to presence of conductive two-dimensional material rGO.

Acknowledgments

The authors are grateful to A.M. Plokhotnichenko for assistance in conducting the low-temperature experiments. This work was supported by the National Academy of Sciences of Ukraine (NASU) (Grant No. 15/19-H within the program “Fundamental Problems of the Creation of New Nanomaterials and Nanotechnology”, Grant No. 07-01-19 and Grant No. 0117U002287). N.V.K. acknowledges support from the NASU: Grant No. 1/H-2019.

1. C. Cheng, S. Li, A. Thomas, N.A. Kotov, and R. Haag, *Chem. Rev.* **117**, 1826 (2017).
2. W. Fan, L. Zhang, and T. Liu, *Graphene–Carbon Nanotube Hybrids for Energy and Environmental Applications* (Series SpringerBriefs in Green Chemistry for Sustainability), Springer, Singapore (2017).
3. K.I. Bolotin, K.J. Sikes, J. Hone, H.L. Stormer, and P. Kim, *Phys. Rev. Lett.* **101,** 096802 (2008).
4. S. Nardecchia, D. Carriazo, M.L. Ferrer, M.C. Gutierrrez, and F. del Monte, *Chem. Soc. Rev.* **42**, 794 (2013).
5. N.F. Mott and E.A. Davis, *Electronic Processes in Non-Crystalline Materials*, Oxford: Clarendon Press, New York (1979).
6. P. Sheng, *Phys. Rev. B* **21**, 2180 (1980).
7. P. Sheng, E.K. Sichel, and J.I. Gittleman, *Phys. Rev. Lett.* **40**, 1197 (1978).
8. C. Gomez-Navarro, R.T. Weitz, A.M. Bittner, M. Scolari, M. Mews, M. Burghard, and K. Kern, *Nano Lett.* **7**, 3499 (2007).
9. A.B. Kaiser, C. Gomez-Navarro, R.S. Sundaram, M. Burghard, and K. Kern, *Nano Lett.* **9**, 1787 (2009).
10. G. Eda, C. Mattevi, H. Yamaguchi, H. Kim, and M. Chhowalla, *J. Phys. Chem. C* **113**, 15768 (2009).
11. B. Muchharla, T.N. Narayanan, K. Balakrishnan, P.M. Ajayan, and S. Talapatra, *2D Materials* **1**, 011008 (2014).
12. G. Venugopal, K. Krishnamoorthy, R. Mohan, and S.-J. Kim, *Mater. Chem. Phys.* **132**, 29 (2012).
13. J. Ma, X. Hou, M. Yu, J. Hua, X. Ren, H. Qiu, and R. Wang, *J. Phys. D* **50**, 435101 (2017).
14. D. Joung and S.I. Khondaker, *Phys. Rev. B* **86**, 235423 (2012).
15. M. Park, S.J. Hong, K.H. Kim, H. Kang, M. Lee, D.H. Jeong, Y.W. Park, and B.H. Kim, *Appl. Phys. Lett.* **111**, 173103 (2017).
16. E. Zion, A. Haran, A.V. Butenko, L. Wolfson, Yu. Kaganovskii, T. Havdala, A. Sharoni, D. Naveh, V. Richter, M. Kaveh, E. Kogan, and I. Shlimak, *Graphene* **4**, 45 (2015).
17. C. Chuang, R.K. Puddy, H.-D. Lin, S.-T. Lo, T.-M. Chen, C.G. Smith, and C.-T. Liang, *Solid State Commun.* **152**, 905 (2012).
18. A.L. Efros and B.I. Shklovskii, *J. Phys. C: Solid State Phys.* **8**, L49 (1975).
19. B.I. Shklovskii and A.L. Efros, *Electronic Properties of Doped Semiconductors*, Springer-Verlag, Berlin (1984).
20. H.-J. Kim, D. Kim, S. Jung, S.N. Yi, Y.J. Yun, S.K. Chang, and D.H. Ha, *J. Phys. Chem. C* **119**, 28685 (2015).
21. V. Skakalova, V. Vretenar, L. Kopera, P. Kotrusz, C. Mangler, M. Mesko, J.C. Meyer, and M. Hulman, *Carbon* **72**, 224 (2014).
22. V.A. Karachevtsev and N.V. Kurnosov, *Fiz. Nizk. Temp.* **45**, 1300 (2019) [*Low Temp. Phys.* **45**, 1109 (2019)].

Порівняння температурних залежностей електропровідності композитної плівки rGO-SWNT та плівок rGO й SWNT

М.В. Курносов, О.С. Лінник, В.О. Карачевцев

В інтервалі температур 25–290 K досліджено температурні залежності електропровідності композитної плівки відновленного оксиду графену з одностінними вуглецевими нанотрубками (rGO-SWNT) та плівки rGO. Обидві плівки було отримано за допомогою вакуумної фільтрації водних суспензій. Виявлено, що температурна залежність провідності подібна залежності провідності у невпорядкованих напівпровідних системах. Показано, що характер температурної залежності провідності різний для плівок чистого rGO, SWNT та їх композиту. Температурні залежності опору плівок $R(T)$ проаналізовано в рамках моделі стрибкової провідності зі змінною довжиною стрибка (VRH), в якій рух електронів обумовлений термоактивованим тунелюванням між локалізованими станами. При аналізі використано двовимірну модель Мотта (Mott 2D VRH) та модель Ефроса–Шкловського (ES VRH). Модель Mott 2D VRH виконувалась для плівки rGO-SWNT в інтервалі температур 25–200 K. При більш високих температурах залежність $R(T)$ було апроксимовано рівнянням Арреніуса, що описує активаційний транспорт електронів при переході з локалізованих станів у делокалізовані. Залежність $R(T)$ плівки rGO відповідала моделі Mott 2D VRH в діапазоні температур від 165 до 290 K, а при більш низьких температурах — моделі ES VRH. З апроксимації залежностей $R(T)$ цими моделями проведено оцінки параметрів електронного транспорту в плівках rGO-SWNT та rGO. Припускається, що нанотрубки в композиті rGO-SWNT виконують функцію провідних містків між листами rGO, що призводить до збільшення провідності в порівнянні з rGO. При цьому власна провідність rGO також впливає на властивості композиту, оскільки двовимірний характер електронного транспорту зберігається, в протилежність з плівкою SWNT, для якої в тому самому інтервалі температур виконувалась тривимірна стрибкова провідність за моделлю Мотта.

Ключові слова: низькотемпературна електропровідність, невпорядковані системи, відновлений оксид графену, одностінні вуглецеві нанотрубки, гібриди відновленого оксиду графену з нанотрубками, стрибкова провідність зі змінною довжиною стрибка.

Сравнение температурных зависимостей электропроводности композитной пленки rGO-SWNT и пленок rGO и SWNT

Н.В. Курносов, А.С. Линник, В.А. Карачевцев

В интервале температур 25–290 K исследованы температурные зависимости электропроводности композитной пленки восстановленного оксида графена с одностенными углеродными нанотрубками (rGO-SWNT) и пленки rGO. Обе пленки были получены с помощью вакуумной фильтрации водных суспензий. Обнаружено, что температурная зависимость проводимости аналогична зависимости проводимости неупорядоченных полупроводниковых систем. Показано, что характер температурной зависимости электропроводности различный для пленок чистого rGO, SWNT и их композита. Температурные зависимости сопротивления пленок $R(T)$ проанализированы в рамках модели прыжковой проводимости с переменной длиной прыжка (VRH), где движение электронов связано с термически активированным туннелированием между локализованными состояниями. При анализе использованы двумерная модель Мотта (Mott 2D VRH) и модель Эфроса–Шкловского (ES VRH). Модель Mott 2D VRH выполнялась для пленки rGO-SWNT в интервале температур 25–200 K. При более высоких температурах зависимость $R(T)$ аппроксимировали уравнением Аррениуса, описывающим активационный транспорт электронов при переходе из локализованных состояний в делокализованные. Зависимость $R(T)$ пленки rGO соответствовала модели Mott 2D VRH в диапазоне температур от 165 до 290 K, а при более низких температурах — модели ES VRH. Из аппроксимации зависимостей $R(T)$ этими моделями выполнены оценки параметров электронного транспорта в пленках rGO-SWNT и rGO. Предполагается, что нанотрубки в композите rGO-SWNT служат в качестве проводящих мостиков между листами rGO, приводя к повышению электропроводности по сравнению с rGO. При этом собственная проводимость rGO также влияет на свойства композита, так как двумерный характер электронного транспорта сохраняется, в противоположность пленке SWNT, для которой в том же интервале температур выполнялась трехмерная прыжковая проводимость по модели Мотта.

Ключевые слова: низкотемпературная электропроводность, неупорядоченные системы, восстановленный оксид графена, одностенные углеродные нанотрубки, гибриды восстановленного оксида графена с нанотрубками, прыжковая проводимость с переменной длиной прыжка.